Impact of the Diurnal Radiation Cycle on Secondary Eyewall Formation

Xiaodong Tang[1], Zhe-Min Tan[1], Juan Fang[1], Y. Qiang Sun[2], and Fuqing Zhang[2]

[1] School of Atmospheric Sciences, Nanjing University, China; [2] Department of Meteorology, The Pennsylvania State University, USA

1. Introduction

- **Secondary eyewall formation (SEF) is a key issue for TC research and forecasting, as it is closely related to both short-term TC intensity change and TC size change.**
- **We demonstrated the impacts of radiation on the size and strength of the mature hurricane Edouard (2014) (Tang and Zhang 2016).**
- **The mechanism by which the solar insolation affects SEF remains unexplored, and this is the focus of the current study.**

2. Experimental setup

➢ **Control run (CNTL):**

- Real diurnal cycle; Hurricane Edouard; integrated from 1200 UTC 11-Sep-2014

➢ **Sensitivity experiments:**

- No solar insolation (**NoSolarRad**); starting at 72 model integration hours of CNTL

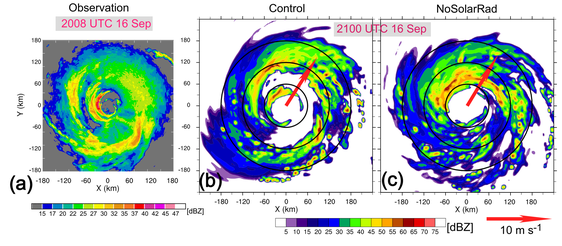

Figure 1: Composite radar reflectivity from (a) aircraft reconnaissance into Hurricane Edouard (2014), and (b) CNTL, and (c) NoSolarRad at a height of 5 km. Red arrows denote vertical shear vectors of averaged environmental wind.

3. Overview of the SEF of Hurricane Edouard (2014)

➢**The critical differences between CNTL and NoSolarRad are the stronger inner rainbands and the lack of a clear moat region in NoSolarRad.**

3.1 Evolution of boundary layer wind (Fig. 2)

➢**CNTL: The double maximum inflow (outflow) regions at the 1-km (2-km) level formed at ~1200 UTC 16 September (Fig. 2b, c).**

➢**CNTL: The secondary maximum of the tangential winds formed at ~1800 UTC 16 September (Fig. 2a).**

➢**NoSolarRad: Heating from stronger inner rainbands outside the RMW in the midtroposphere → increasing (reducing) low-level tangential wind outside (near and inside) the RMW → outward expansion of the RMW (Fig. 2d).**

➢**NoSolarRad: The maximum radial inflow was farther out from the RMW during the period from 1800 UTC 15 September to 0600 UTC 16 September (Fig. 2e), without a continuous secondary maximum of 2-km outflow (Fig. 2f).**

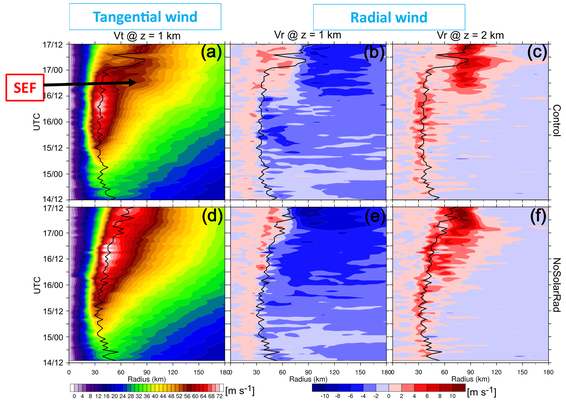

Figure 2: Hovmöller plots of azimuthal-mean tangential velocity at a height of 1 km and radial velocity at heights of 1 and 2 km for (a)–(c) CNTL and (d)–(f) NoSolarRad. The superposed black lines denote the RMW at 1 km.

3.2 Evolution of vertical velocity (Fig. 3)

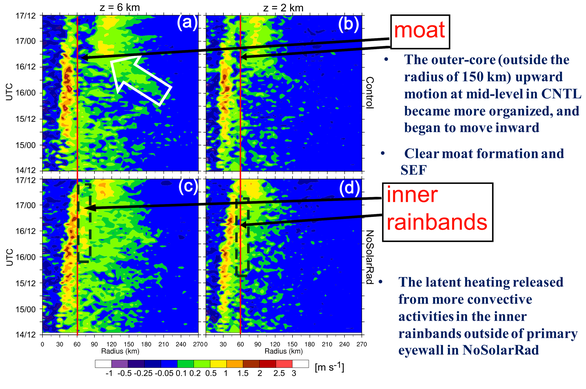

- **The outer-core (outside the radius of 150 km) upward motion at mid-level in CNTL became more organized, and began to move inward**
- **Clear moat formation and SEF**
- **The latent heating released from more convective activities in the inner rainbands outside of primary eyewall in NoSolarRad**

Figure 3: Hovmöller plots of azimuthal mean vertical velocity at heights of 6 and 2 km for (a)–(b) CNTL and (c)–(d) NoSolarRad. The vertical red lines show key radial distances.

4. Radiative effects on SEF

4.1 Moat formation

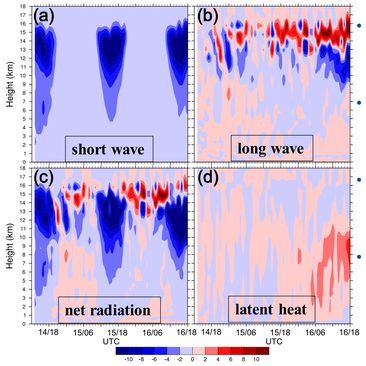

- **The net radiative heating in CNTL is much stronger due to the solar insolation at daytime.**
- **Less conducive for deep moist convection in CNTL**
- **Less diabatic heating due to suppressed convection in CNTL**
- **Difference: 0.5–1 K/day at the top of the boundary layer**

Figure 4: Height–time plot of NoSolarRad minus CNTL difference of (a) shortwave radiative heating, (b) longwave radiative heating, (c) net radiative heating, and (d) latent heating between 60 and 75 km radius from 1300 UTC 14 September to 1800 UTC 16 September 2014. The units are 10^{-5} K/s for (a)–(c) and 10^{-3} K/s for (d).

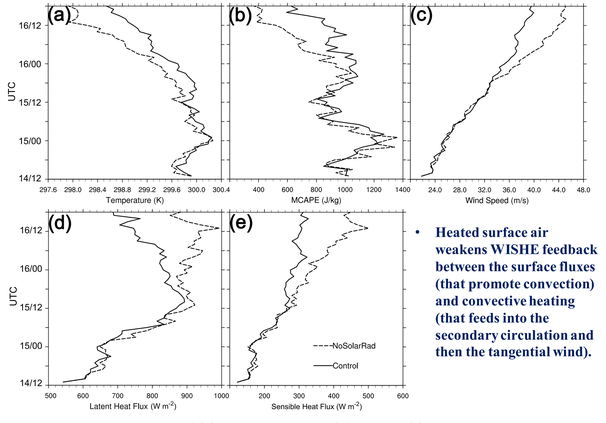

- **Heated surface air weakens WISHE feedback between the surface fluxes (that promote convection) and convective heating (that feeds into the secondary circulation and then the tangential wind).**

Figure 5: Evolution of (a) 2-m temperature, (b) MCAPE, (c) 10-m wind speed, and surface fluxes of (d) latent heat and (e) sensible heat averaged between 60 and 75 km radius for CNTL and NoSolarRad.

4.2 Balanced aspects of SEF

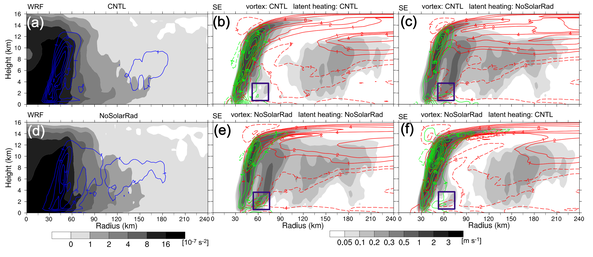

Figure 6: Radius–height cross-sections of the 2-hour azimuthal-mean of the inertial stability parameter I^2 (shading) and latent heating (blue contours, unit: 10^{-3} K/s) from WRF output in (a) CNTL and (d) NoSolarRad, and of vertical velocity (shading), radial velocity (red contours, unit: m/s), and the combined contribution of radial advection of absolute vorticity and vertical advection of tangential wind to the tangential wind tendency (green contours, 10^{-3} m s^{-2}) from Sawyer-Eliassen model calculations using (b) the background vortex structure and diabatic heating from CNTL, (c) the background vortex structure of CNTL, diabatic heating from NoSolarRad, (e) the background vortex structure and diabatic heating from NoSolarRad, and (f) the background vortex structure of NoSolarRad and diabatic heating from CNTL. The period is from 0500 to 0700 UTC 16 September 2014.

5. Concluding remarks

- **Moat region is highly sensitive to the solar shortwave radiative heating mostly in the mid- to upper-level at daytime, which leads to a net stabilization effect and suppresses convective development.**
- **The heated surface air weakens WISHE feedback between the surface fluxes (that promote convection) and convective heating (that feeds to the secondary circulation and then the tangential wind).**
- **NoSolarRad: without solar radiation, active inner rainband, suppressed primary eyewall, no moat, no SEF**
- **The radiation-induced absence of latent heating is more important on moat formation in the early stage of SEF.**

6. Further reading

- **Tang, X., and F. Zhang, 2016: Impacts of the Diurnal Radiation Cycle on the Formation, Intensity and Structure of Hurricane Edouard (2014), *J. Atmos. Sci.*, 73, 2871-2892.**
- **Tang, X. et al, 2017: Impact of the Diurnal Radiation Cycle on Secondary Eyewall Formation, *J. Atmos. Sci.*, 74, 3079-3098.**